

中国激光

基于 Parity-Time 对称耦合微腔的血糖传感器

叶思放¹, 方云团^{1,2*}

¹ 江苏大学计算机科学与通信工程学院, 江苏 镇江 212013;

² 江苏大学江苏省工业网络安全技术重点实验室, 江苏 镇江 212013

摘要 为设计新型光学生物传感器, 本课题组构造了基于 Parity-Time (PT) 对称的耦合谐振腔系统, 用于实现对人体血糖浓度的测量。通过结构优化, 使系统达到 PT 对称极点状态, 然后利用极点状态下透射率对血糖折射率极其敏感的特性, 将对血糖浓度的测量转化为对系统透射率的测量, 从而达到血糖传感的目的。本文研究了两种传感方式: 一是固定特定极点处的频率, 测量系统在不同血糖浓度下的透射率; 二是在极点附近的频率范围内扫描, 测量特定血糖浓度下透射率的峰值。血糖质量浓度为 20~182 mg/dL 时, 第二种方式下传感器的灵敏度均高于第一种方式; 当血糖质量浓度高于 182 mg/dL 时, 第一种方式在 1466.40 THz 频率下的灵敏度要比第二种方式高。可以将本文对血糖浓度的传感方式推广到对其他生物样本的测量上。

关键词 传感器; PT 对称结构; 耦合谐振腔; 极点; 灵敏度

中图分类号 TP212.3 文献标志码 A

doi: 10.3788/CJL202249.0310002

1 引言

随着生活水平的不断提升, 不少人在日常生活中摄入了过多的能量, 使得糖尿病的发病率逐年增加。肾衰竭、心脏病等很多疾病都会引起血糖异常, 所以, 血糖检测越来越受到人们的重视, 进而高性能血糖传感装置的研制具有重要意义。

利用光子晶体设计的传感器已被广泛应用到生物学和医学领域。很多研究者基于不同血糖浓度对光学系统的影响设计了具有高灵敏度的血糖传感器^[1-5], 这些传感器大多从血糖浓度与其折射率间的关系出发, 利用折射率变化引起的传感器透射峰的移动进行传感。例如文献[1-3]的作者在一维光子晶体缺陷中引入待检测的血液后发现, 缺陷模式在带隙中的位置会随着血糖浓度的变化而变化, 因此他们将缺陷模式在带隙中位置的变化作为检测血糖浓度的手段。Mohamed 等^[4]同样利用二维光子晶体设置缺陷, 然后在缺陷中填充待检测的血液, 由于缺陷共振模式的波长也会随血糖浓度的变化而变化, 因此也可以检测血糖的浓度。Yeh^[5]通过激光干涉仪测得的血糖样品的折射率来间接推导血糖浓

度。上述检测方法在血糖浓度变化较大时比较有效, 但是在血糖浓度变化较小时, 缺陷模式波长的变化或者样品折射率的变化很小, 很难被仪器识别, 导致传感的精度和灵敏度受到限制。近年来, 增益和损耗介质特定分布的光学 Parity-Time(PT)对称结构^[6-9]在新型光子器件的设计方面显示出独特优势, 为突破传统光子器件的技术瓶颈提供了全新的解决方案^[10]。具有 PT 结构的典型器件有高灵敏传感器^[11]、激光吸收器^[12-13]、光隔离器^[14]、放大和吸收的功能转换器^[15]和无线电能传输器^[16]等。与传统的光子晶体传感器利用峰值的移动进行传感不同, 本课题组将 PT 对称耦合微腔结构透射率的变化作为传感指标。PT 对称耦合微腔结构在 PT 对称破缺态存在一些离散的极点, 极点处结构散射矩阵的两个本征值互为倒数, 它们分别对应受激放大模式(透射和反射趋于无穷大)和相干完美吸收模式^[12-13]。本课题组在 PT 对称耦合微腔结构的耦合层中填充待测血液, 进行血糖浓度的测量。血糖浓度的变化会使血液的折射率发生变化, 进而使整个结构的透射率发生变化。本课题组通过结构优化, 使结构处于 PT 对称的极点状态, 这样血糖浓度的

收稿日期: 2021-04-20; 修回日期: 2021-05-19; 录用日期: 2021-06-18

通信作者: *fang_yt1965@sina.com

微小变化就会使传感器的透射率发生明显变化,解决了传统血糖传感器测量精度受限的难题,为测量血糖浓度提供了一种新方式。本文传感器的设计思想不仅仅局限于血糖浓度的测量,也为其他生物样本的检测提供了一种普适方法。

2 模型设计和模式分析

传感器理论模型如图1所示。整体结构可以表示为PAGA₁LAP。其中:P层为一对棱镜,棱镜的底角为 θ ,折射率为 $n_p=3.48$;A层为空气层,厚度为 $d_A=400\text{ nm}$,折射率为 $n_A=1.00027$;G层和L层分别是增益层和损耗层,构成两个耦合谐振腔,对应的厚度分别为 $d_G=d_L=1500\text{ nm}$,增益层对应的折射率是 $n_G=3.205-i\tau$,损耗层对应的折射率是 $n_L=3.205+i\tau$,其中 τ 是增益和损耗系数。整体结构符合PT对称要求:折射率实部偶对称,虚部奇对称^[6]。中间的A₁层是耦合层,对应的厚度为 $d_{A_1}=400\text{ nm}$,A₁层填充的是待测物体。整个系统的输入端是信号发生器,用于发射单一或者某一范围频率的电磁波;输出端接的是光电传感器,用于将透射光的强度转化为电流信号。增益和损耗材料的选择参考了文献[15],将掺杂量子阱的半导体InGaAsP作为增益介质层,在增益介质层上覆盖吸收介质Cr/Ge形成损耗层。

传感器通过透射谱来测定待测物理量,因此需要

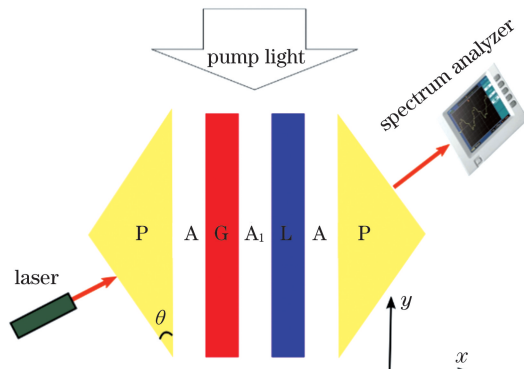


图1 结构示意图(P是一对棱镜,G和L分别是增益和损耗谐振腔,A是空气层,A₁是耦合层,入射方向垂直于棱镜外表面)

Fig. 1 Schematic of designed structure (the symbol P refers coupling prism. G and L denote gain and loss resonators, respectively. A denotes air layers. A₁ is coupling layer that is full of detected material. The prism has a base angle $\theta = 30^\circ$. The light incident direction is perpendicular to external interface of the prism)

计算出整体结构的透射率。对于有限周期的一维层状结构,可以用传统的传输矩阵法进行计算^[17-18]。又因为所提结构的主体是两个耦合谐振腔,因此模式的演变可以用耦合模公式来分析^[19]。耦合模公式为

$$\begin{cases} \frac{da_1}{dt} = -i(\omega_0 + ig)a_1 - i\kappa a_2, \\ \frac{da_2}{dt} = -i(\omega_0 + i\gamma)a_2 - i\kappa a_1, \end{cases} \quad (1)$$

式中: a_1 和 a_2 分别为谐振腔G层和L层的幅值; ω_0 是单个G层和L层在 $\tau=0$ 时的谐振频率; g 和 γ 分别为增益系数和损耗系数,由 τ 决定($g=\tau$, $\gamma=-\tau$); κ 是耦合系数。假设整个系统具有 $\exp(-i\omega t)$ 的形式,其中 ω 是耦合系统的本征频率, t 是时间,则有

$$\frac{d}{dt} \begin{bmatrix} a_1 \\ a_2 \end{bmatrix} = -i\omega \begin{bmatrix} a_1 \\ a_2 \end{bmatrix}. \quad (2)$$

结合(1)式和(2)式可以得到本征频率的矩阵方程为

$$\begin{bmatrix} (\omega_0 + ig) & \kappa \\ \kappa & (\omega_0 + i\tau) \end{bmatrix} \begin{bmatrix} a_1 \\ a_2 \end{bmatrix} = \omega \begin{bmatrix} a_1 \\ a_2 \end{bmatrix}. \quad (3)$$

根据PT对称的性质,有 $g=-\gamma$,则可以得到(3)式的解为

$$\omega = \omega_0 \pm \sqrt{\kappa^2 - g^2}. \quad (4)$$

当 $\kappa > g$ 时,对应的 ω 的解为两个不相等的实数;当 $\kappa < g$ 时,则对应的解为一对共轭复数,此时为PT对称破缺态;当 $\kappa = g$ 时,是PT对称态和PT对称破缺态的临界点(称为奇点),对应的解为两个相等的实数 ω_0 。根据文献[12-13],在PT对称结构破缺态下,结构散射矩阵本征值与频率的关系曲线上存在一些离散的极点,极点处散射矩阵的两个本征值互为倒数,它们分别对应受激放大模式(透射和反射趋近无穷大)和相干完美吸收模式。

先假设A₁层填充的是空气,同时先考虑 $\tau=0$ 。基于传输矩阵法利用MATLAB编程计算可以得到如图2所示的结果。图中出现了两个相邻的透射率

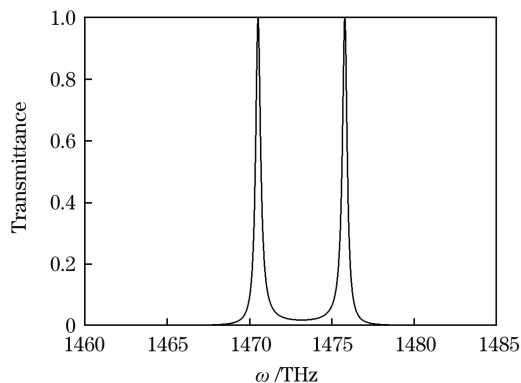


图2 $\tau=0$ 时所对应的透射谱

Fig. 2 Transmission spectrum at $\tau=0$

接近 1 的透射峰,透射峰对应的频率即为两个耦合模式的频率,这与(4)式中 $g=0$ 的情况相对应,即有两个不相等的实数解。

接下来,逐渐增大 τ 的值,可以得到一系列透射谱,如图 3 所示。对比图 3(a)、(b)与图 2 可知,增大 τ 时,两个透射峰逐渐靠近。这是由于 τ 的增大会导致 g 增大,使耦合程度不断增强,(4)式中的两个实数解越来越接近。当 $\tau=0.00385$ 时,得到

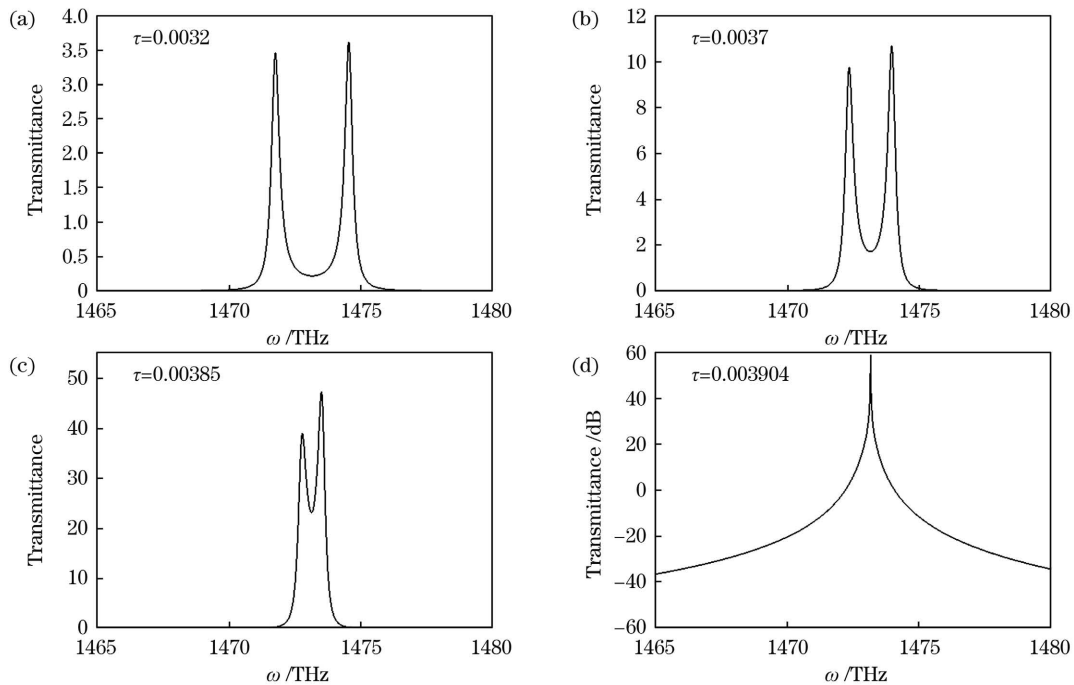


图 3 τ 值逐渐增大时对应的透射谱

Fig. 3 Transmission spectra as the value of τ gradually increases

3 传感机制和结果分析

3.1 传感机制

要测量血糖浓度,需要将图 1 中的 A_1 层填充血液,把对血糖浓度的测量转化为对透射率的测量。因此,需要知道血糖浓度与折射率之间的关系。影响血糖折射率的因素有很多,但血糖浓度是最主要的因素,这里忽略其他因素的影响,把血糖折射率和血糖浓度看作一一对应的关系。血糖浓度和折射率之间的关系可由经验公式^[5]给出。经验公式为

$$n_{A_1} = 1.33230545 + 0.00011889c, \quad (5)$$

式中, c 是血液中的葡萄糖的质量浓度,单位是 g/L, c 的取值范围是 0~5 g/L。然而,在实际测量中,常用的血糖质量浓度的单位是 mg/dL,所以将(5)式进行转换。新的表达式为

$$n_{A_1} = 1.33230545 + 0.0000011889p, \quad (6)$$

式中: p 表示血糖质量浓度,单位为 mg/dL。在现实

图 3(c)所示的结果,两个透射峰进一步靠近。继续增大 τ 值,两个透射峰完全合并,透射率逐渐增大,此时对应 $\kappa < g$,两个频率实部合并,频率变为复数,系统进入 PT 对称破缺态。当 $\tau = 0.003904$ 时,如图 3(d)所示,透射率出现跃升,系统的透射率达到 60 dB,这就是系统的极点状态。在该状态下,系统的透射率对背景和结构参数的变化极其敏感,从而为传感器设计创造了条件。

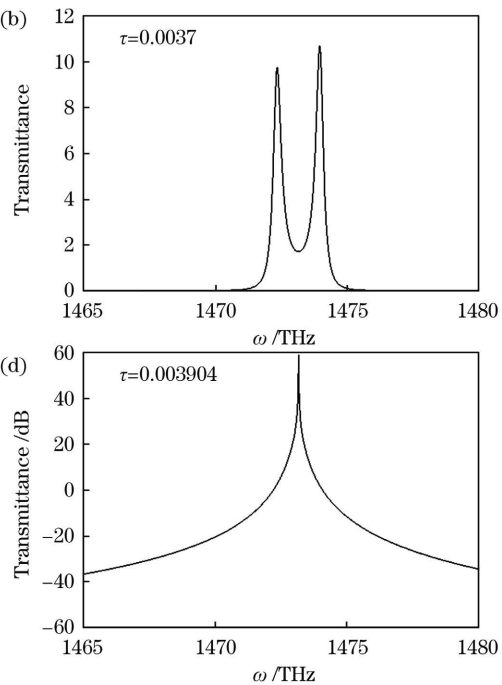


图 4 血糖质量浓度与其折射率之间的关系

Fig. 4 Relationship between blood glucose mass concentration and its refractive index

由图 4 可知,当血糖质量浓度在 20~200 mg/dL 之间变化时,血液的折射率与血糖浓度呈线性关系。

虽然折射率的变化范围很小,但这个变化足以给 PT 对称结构的极点传输带来很大变化。在图 4 中选取 $P_1(52.18, 1.3323675)$ 、 $P_2(73.44, 1.3323928)$ 、 $P_3(87.20, 1.3324091)$ 、 $P_4(106.40, 1.3324320)$ 这几个点来分析和确定传感器的传感方式。

根据图 4 选取 4 个血糖浓度,取 $\tau=0.006701$,可以得到 4 个血糖浓度对应的透射谱。为了方便分析,将 4 个透射谱放到一张图中,如图 5 所示。当血糖质量浓度为 52.18 mg/dL 时,对应的峰值位于 1466.508 THz ,峰值大小为 63.6 dB ;当血糖质量浓度为 73.44 mg/dL 时,对应的峰值位于 1466.511 THz ,峰值大小为 49.29 dB ;当血糖质量浓度为 87.2 mg/dL 时,对应的峰值位于 1466.512 THz ,峰值大小为 47.555 dB ;当血糖浓度为 106.40 mg/dL 时,对应的峰值位于 1466.513 THz ,峰值大小为 45.59 dB 。对数据进行分析后可知,随着血糖浓度不断升高,传感器的峰值逐渐减小,且峰值所在位置不断右移。极点的形成与结构参数密切相关。血糖浓度升高导致微腔层折射率和微腔共振波长变大,偏离了极点形成条件,从而导致峰值右移,透射率下降。理论上,可以利用峰值位置来测量血糖浓度,然而,由于折射率的变化幅度很小,因此引起的峰值位置的移动也很小,导致传感器的灵敏度不高。PT 对称结构的极点效应导致不同血糖浓度下系统的透射率有显著差异,因此,本课题组考虑通过透射率的大小来测量血糖浓度。

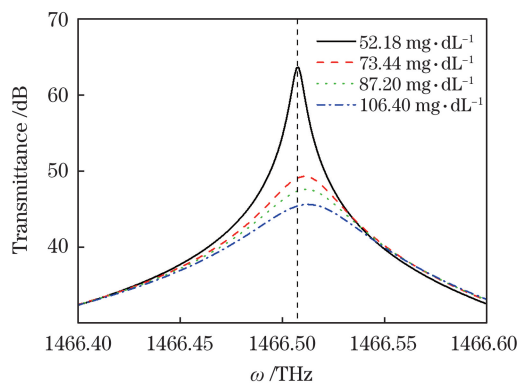


图 5 不同血糖质量浓度对应的透射谱

Fig. 5 Transmission spectra corresponding to different blood glucose mass concentrations

3.2 两种传感机制的结果和分析

从图 5 可知,利用透射率的大小来设计传感器可以有两种方式:第一种是固定入射波频率,测量每个血糖浓度在该频率下对应的透射率;第二种是测量每个血糖浓度在某一频率范围内对应的最大透射率,即图 5 中每条曲线峰值的大小。下面通过具体

的数值分别给出这两种传感机制的结果。

对于第一种方式,首先选取图 5 中黑色实线最高峰所在的频率 1466.508 THz ,计算系统透射率与血糖浓度之间关系的曲线,计算结果如图 6 所示。由图 6 可知,当血糖浓度在 $20 \sim 200 \text{ mg/dL}$ 之间时,系统的透射率随着血糖浓度的增大而不断减小,且与血糖浓度是一一对应关系。这种关系说明可以通过系统透射率的大小来测量血糖浓度。

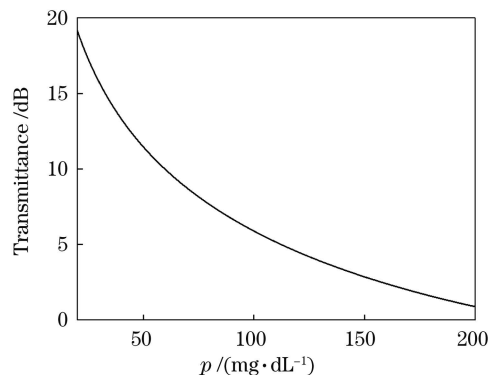


图 6 固定频率传感方式下透射率随血糖质量浓度的变化

Fig. 6 Dependence of transmittance on blood glucose mass concentration with the fixed frequency

灵敏度是衡量传感器性能的重要指标,本文计算灵敏度的方法如图 7(a)所示。以计算血糖质量浓度为 $p_0=74 \text{ mg/dL}$ 时的相对灵敏度为例,相对灵敏度的计算公式为 $S=\Delta T/T_0$,其中 T_0 表示血糖浓度为 p_0 时对应的传感器透射率, ΔT 表示血糖质量浓度与 p_0 相差 1 mg/dL 时传感器透射率差值的绝对值。相对灵敏度 S 表示血糖质量浓度改变 1 mg/dL 时引起的传感器透射率的变化。入射频率为 1466.508 THz 时,传感器的灵敏度曲线如图 7(b) 所示。由图 7(b) 可知,传感器在 $50 \sim 150 \text{ mg/dL}$ 时的灵敏度较低,且变化缓慢,在小于 50 mg/dL 和大于 150 mg/dL 时的灵敏度较大。由图 7(b) 还可以看到,此参数下的传感器在高血糖浓度和低血糖浓度下均具有更好的灵敏度表现。

接下来考虑入射波频率对第一种传感方式灵敏度的影响。图 8 给出了在入射波频率为 $1466.40, 1466.45, 1466.47, 1466.50 \text{ THz}$ 的情况下,传感器对应的灵敏度。由图 8 可知:在血糖质量浓度低于 150 mg/dL 时,所有曲线几乎重叠,入射波频率对传感器的灵敏度影响很小;而血糖质量浓度在 $150 \sim 200 \text{ mg/dL}$ 时,总体灵敏度值随血糖浓度增加而迅速变大,但曲线分离度较大,说明灵敏度对频率敏感。在相同的条件下,入射波频率越小,灵敏度越高。因此,在这种设计方式下可以选择低入射波

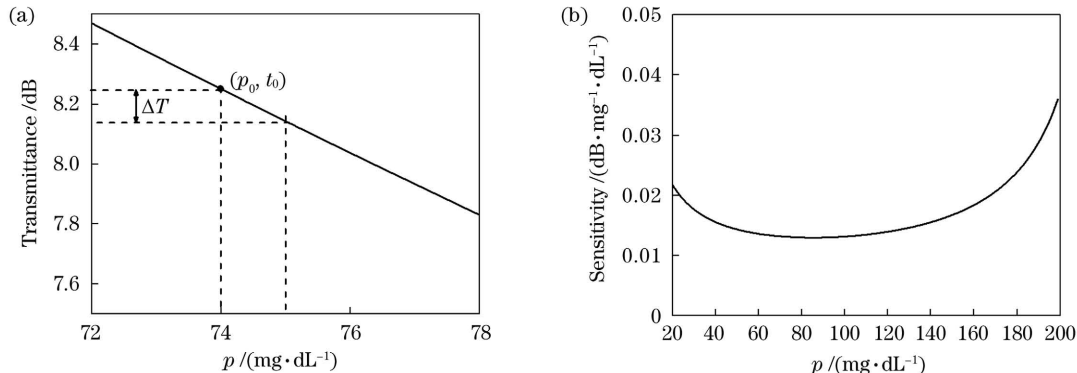


图7 传感器灵敏度的计算。(a)相对灵敏度的计算方法;(b)入射波频率为1466.508 THz时对应的灵敏度

Fig. 7 Calculation of sensor sensitivity. (a) Calculation method of relative sensitivity; (b) sensitivity corresponding to incident wave frequency of 1466.508 THz

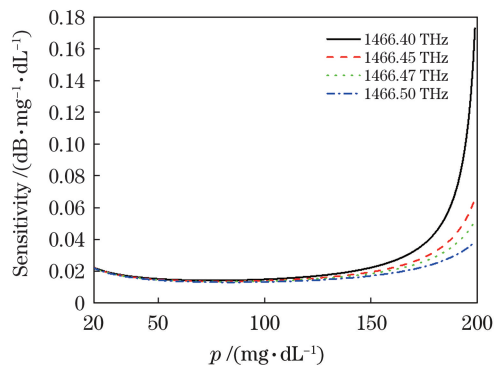


图8 不同入射波频率下传感器对应的灵敏度

Fig. 8 Sensitivity of sensor at different incident wave frequencies

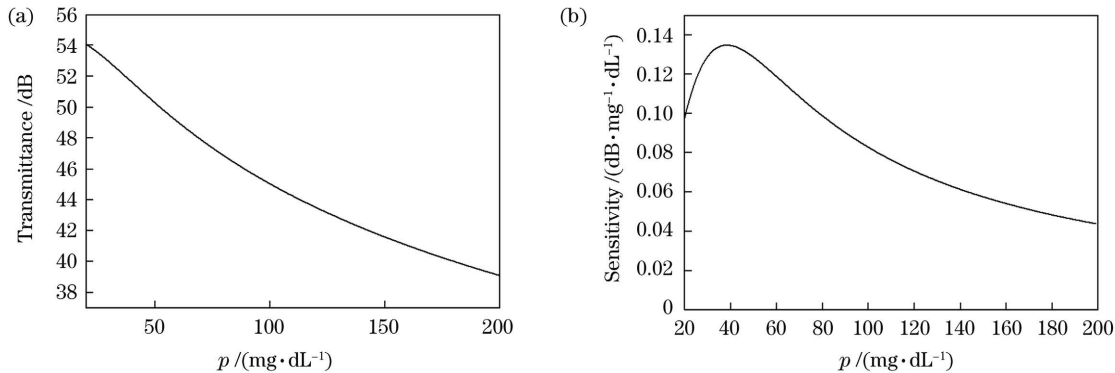


图9 按峰值大小进行传感时的透射谱和灵敏度曲线。(a)透射谱;(b)灵敏度曲线

Fig. 9 Transmission spectrum and sensitivity curve of peak value sensing. (a) Transmission spectrum; (b) sensitivity curve

对比两种设计方式下传感器的表现可以发现,除了在1466.4 THz、182~200 mg/dL范围内第一种方式下的传感器灵敏度大于第二种方式外,第二种方式下的传感器灵敏度都要大于第一种传感方式,特别是在20~80 mg/dL范围内,第二种方式的灵敏度要远大于第一种方式。这是因为,血糖浓度越低,透射峰值越大(如图5所示),极点效应越明显,因此基于极点峰值检测的第二种方式的灵敏度要更

频率,即1466.40 THz。

对于第二种方式,选择入射波的扫描频率范围为1465~1475 THz,得到的不同血糖浓度下峰值透射率曲线如图9(a)所示。从图9(a)中可以发现,整个曲线随血糖浓度增加呈下降的趋势。值得注意的是,该曲线近似为一条直线,这样的曲线便于拟合,特别有利于传感器的定标。同样,计算出了这种设计方式下传感器的灵敏度,计算结果如图9(b)所示。由图9(b)可以看出,这种设计方式下传感器的灵敏度在20~38 mg/dL时逐渐增大,然后随着血糖浓度继续增大而逐渐降低。在此方式下,传感器在38 mg/dL附近的灵敏度最高。

高;而在高血糖质量浓度范围(182~200 mg/dL)内,透射峰值变小,极点效应变弱,第二种方式的灵敏度变低。第一种方式的频率固定在1466.40 THz,是低浓度下的极点频率,因此当浓度增大时,透射率偏离极点位置,变化更明显,灵敏度更高;第二种方式是检测透射峰值,需要较大的频率扫描范围和较高的扫描精度,增大了复杂度。总的来说,这两种传感方式各有优缺点,如果检测葡萄糖质量浓度大(大于

182 mg/dL)的血液样本,可以选择第一种方式,而如果检测低葡萄糖浓度的血液样本而且对灵敏度要求较高时,可以选择第二种方式。

对于第二种方式,为了在测量范围内找到任意血糖浓度与系统透射率的解析关系,先将图9(a)所示曲线的横纵坐标调换,然后利用MATLAB进行拟合,拟合多项式的阶数为4。拟合结果如图10所示,可见,拟合结果与原始曲线基本吻合。拟合多项式的表达式为

$$p(T) = -0.0005250T^4 + 0.06621T^3 - 1.9060T^2 - 51.3718T + 2391, \quad (7)$$

式中: p 表示血糖质量浓度,单位是mg/dL; T 表示体系的透射率,单位是dB。在实际使用过程中,可以利用测量的透射率 T 直接根据(7)式计算得到血糖浓度。从图10可以看出,血糖浓度和透射率的变化关系是连续曲线,因此理论上可以测量出任意小的血糖浓度的变化。但由于光信号要转化为可计量的电流信号,所以实际测量精度还取决于使用的光电传感器的分辨率。另外,极点频率选择的准确与否也是影响精度高低的一个因素。

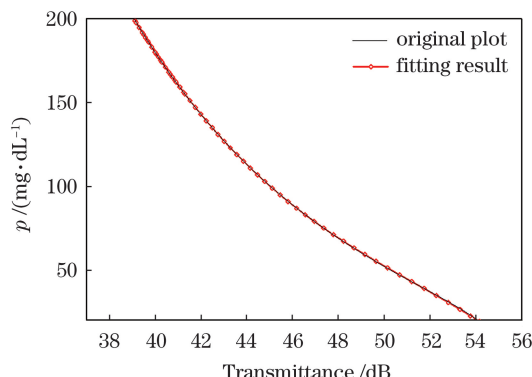


图10 原始数据与拟合结果

Fig.10 Original data and fitting curve

4 结 论

本课题组利用PT对称结构的极点效应设计了一个血糖浓度传感的理论模型。与传统传感器使用频谱位置进行传感不同,该模型将频谱透射率的大小作为传感的手段,具有高精度和高灵敏度的特征。虽然所设计的模型针对的是血糖传感,但实际上它可以推广到一般生物样本,包括各种病变细胞的传感上。因此,本研究为生物传感提供了一种新的普适方法。

参 考 文 献

- [1] Bouzidi A, Bria D, Falyouni F, et al. A biosensor based on one-dimensional photonic crystal for monitoring blood glycemia [J]. Journal of Materials and Environmental Sciences, 2017, 8 (11): 3892-3896.
- [2] Areed N F F, Hameed M F O, Obayya S S A. Highly sensitive face-shaped label-free photonic crystal refractometer for glucose concentration monitoring [J]. Optical and Quantum Electronics, 2016, 49(1): 1-12.
- [3] Elsayed H A, Mehaney A. A new method for glucose detection using the one dimensional defective photonic crystals [J]. Materials Research Express, 2018, 6(3): 036201.
- [4] Mohamed M S, Hameed M F O, Areed N F, et al. Analysis of highly sensitive photonic crystal biosensor for glucose monitoring [J]. ACES Journal, 2016, 31 (7): 836-842.
- [5] Yeh Y L. Real-time measurement of glucose concentration and average refractive index using a laser interferometer [J]. Optics and Lasers in Engineering, 2008, 46(9): 666-670.
- [6] Özdemir S K, Rotter S, Nori F, et al. Parity-time symmetry and exceptional points in photonics [J]. Nature Materials, 2019, 18(8): 783-798.
- [7] Sone K, Ashida Y, Sagawa T. Exceptional non-Hermitian topological edge mode and its application to active matter [J]. Nature Communications, 2020, 11(1): 5745.
- [8] Hassani Gangaraj S A, Monticone F. Topological waveguiding near an exceptional point: defect-immune, slow-light, and loss-immune propagation [J]. Physical Review Letters, 2018, 121 (9): 093901.
- [9] Zhao H, Qiao X D, Wu T W, et al. Non-Hermitian topological light steering [J]. Science, 2019, 365 (6458): 1163-1166.
- [10] Qi B K, Chen H Z, Ge L, et al. Parity-time symmetry synthetic lasers: physics and devices [J]. Advanced Optical Materials, 2019, 7(22): 1900694.
- [11] Hodaei H, Hassan A U, Wittek S, et al. Enhanced sensitivity at higher-order exceptional points [J]. Nature, 2017, 548(7666): 187-191.
- [12] Chong Y D, Ge L, Stone A D. PT-symmetry breaking and laser-absorber modes in optical scattering systems [J]. Physical Review Letters, 2011, 106(9): 093902.
- [13] Ge L, Chong Y D, Stone A D. Conservation relations and anisotropic transmission resonances in one-dimensional PT-symmetric photonic heterostructures [J]. Physical Review A, 2012, 85(2): 023802.
- [14] Chang L, Jiang X S, Hua S Y, et al. Parity-time

- symmetry and variable optical isolation in active-passive-coupled microresonators [J]. *Nature Photonics*, 2014, 8(7): 524-529.
- [15] Wong Z J, Xu Y L, Kim J, et al. Lasing and anti-lasing in a single cavity[J]. *Nature Photonics*, 2016, 10(12): 796-801.
- [16] Assawaworrarit S, Yu X F, Fan S H. Robust wireless power transfer using a nonlinear parity-time-symmetric circuit [J]. *Nature*, 2017, 546 (7658): 387-390.
- [17] Zhang Y C, Jiang X M, Xia J, et al. Tunable high sensitivity temperature sensor based on transmittance changes of parity-time symmetry structure [J]. *Chinese Journal of Lasers*, 2018, 45(7): 0710002.
- 张亦驰, 江晓明, 夏景, 等. 基于宇称-时间对称结构透射率变化的可调高灵敏度温度传感器[J]. 中国激光, 2018, 45(7): 0710002.
- [18] Wang Y Y, Xia J, Fang Y T. Unique non-reciprocal mode with a parity-time symmetric structure under magneto-optic effects[J]. *Chinese Journal of Lasers*, 2018, 45(12): 1213001.
- 王誉雅, 夏景, 方云团. 磁光效应下 PT 对称结构独特的非互易传输模式[J]. 中国激光, 2018, 45(12): 1213001.
- [19] Fang Y T, Li X X, Xia J, et al. Sensing gases by the pole effect of parity-time symmetric coupled resonators[J]. *IEEE Sensors Journal*, 2019, 19(7): 2533-2539.

Blood Glucose Sensor Based on Parity-Time Symmetry Coupled Cavities

Ye Sifang¹, Fang Yuntuan^{1,2*}

¹ School of Computer Science and Telecommunication Engineering, Jiangsu University, Zhenjiang,
Jiangsu 212013, China;

² Jiangsu Key Laboratory of Security Tech. for Industrial Cyberspace, Jiangsu University, Zhenjiang,
Jiangsu 212013, China

Abstract

Objective With the continuous improvement of living standards, excessive energy intake increases the rate of diabetes yearly. Additionally, kidney failure, heart disease, and many other diseases can cause blood glucose abnormalities. Therefore, paying attention to the detection of blood glucose and the design of glucose sensors with high performance become essential. Sensors based on photonic crystals (PCs) are widely used in biology and medicine. Most of these sensors are based on the relationship between blood glucose concentration and its refractive index. The change in the refractive index will cause the movement of the transmission peak of PCs. Thus, people can detect blood glucose concentration by measuring the movement of the transmission peak. However, the movement of the transmission peak is too little for detecting with a small change in the refractive index. Thus, the small change in blood glucose concentration is not easily detected with PC sensors. To solve this problem, a coupled-resonator system based on Parity-Time (PT) symmetric configuration is constructed to measure blood glucose concentration. The polar effect of the PT-symmetric structure will be excited through structural optimization. On the pole state, the PT-symmetric structure can achieve huge transmittance and reflectance and is extremely sensitive to the change of structural parameters. When the blood is filled with the coupling layer, the change in blood glucose concentration changes the refractive index; thus, changing the sensor's transmittance. On the pole state, the transmittance of the sensor changes, even for the small change in blood glucose concentration, the transmittance of the sensor changes obviously. This can solve the problem of limited sensitivity and accuracy of traditional blood glucose sensors. It also provides an approach for measuring blood glucose concentration. The design idea of this sensor is not limited to the measurement of blood glucose concentration and provides a universal method for detecting other organisms.

Methods The designed model of the sensor is shown in Fig. 1. The overall structure was expressed as PAGA₁LAP. The two layers P were a pair of coupled prisms with the base angle θ and the refractive index 3.48. Layer A was the air layer with a thickness of $d_a = 400$ nm and the refractive index of $n_A = 1.00027$. Layers G and L were gain and loss layers, which constitute two-coupled resonators with the same thickness of 1500 nm. The refractive indexes of layers G and L were $n_G = 3.205 - i\tau$ and $n_L = 3.205 + i\tau$, where τ was the gain and loss coefficient. The overall structure met the requirements of the PT-symmetry that the real part of the refractive index was even symmetry and

the imaginary part was odd symmetry. The middle layer A_1 was filled with the object to be measured. The input light was incident on the left prism, and a total reflection occurred on its inner interface. The evanescent waves entered the two-coupled resonators and achieved resonance transmission. The output through the right prism was connected with a photoelectric sensor, which converted the intensity of transmitted light into the current signal for recording. Semiconductor InGaAsP doped with quantum well was used as the gain dielectric layer, and Cr/Ge was covered on the gain dielectric layer to form the loss layer. The transfer matrix method was used to calculate the transmittance and reflectance of the structure. To achieve the purpose of blood glucose sensing, measurement of blood glucose concentration was transformed into the measurement of the system transmittance.

Results and Discussions First, we assume that layer A_1 was filled with air. The result in Fig. 2 shows that there are two adjacent transmission peaks with transmittance near 1 corresponding to the two-coupled modes. With $\tau = 0.003904$, the two peaks merges into one peak, and the peak value undergoes a jump zoom up to 60 dB. This is the pole state. Next, we assume that layer A_1 is filled with blood with different glucose concentrations and the corresponding transmittance is calculated. The results are shown in Fig. 5. We choose $\tau = 0.006701$ to excite the pole effect for the new medium in layer A_1 . The change in the blood glucose concentration leads to different peak values and positions. In this study, we investigate two sensing methods. One is to fix the frequency around a specific pole to measure the system transmittance under different blood glucose concentrations. The other is to detect the peak value corresponding to a specific blood glucose concentration by scanning the transmission spectrum near the pole. The sensing results and the corresponding sensitivities for the two methods are shown in Figs. 7 and 9, respectively. When the blood glucose concentration is 20–182 mg/dL, the sensor's sensitivity in the second method is higher than that in the first method. However, when the blood glucose concentration is higher than 182 mg/dL, the sensor's sensitivity in the first method is higher than that in the second method. If the sensor detects blood glucose with a high concentration, the first method can be selected. However, the second method can be selected if the sensor detects blood glucose with low concentration and requires high sensitivity.

Conclusions In this study, we design a theoretical model of glucose concentration sensor using the pole effect of the PT-symmetric structure. Unlike the traditional sensor, the designed model does not use spectrum positions as the sensing mechanism but uses transmittance detection as the sensing method. The new sensing mechanism has high precision and sensitivity. Although our model is for blood glucose sensing, it can be extended to general biomaterial sensing, including sensing various diseased cells. Therefore, this study provides a new universal method for biosensors.

Key words sensors; Parity-Time symmetric structure; coupled resonators; pole; sensitivity